

Advancements in hydroacoustic signal processing at CTBT IDC during the past two decades and plans for the future

P.L. Nielsen, R. Le Bras, P. Mialle, N. Kushida, P. Bittner and M. Kalinowski
CTBTO

O3.7-283



OUTLINE

- Origin of what became the CTBT IDC automatic processing algorithm
- Highlights in advancements of automatic hydroacoustic data processing over 25 years
- Future hydroacoustic data processing capabilities. Near and long-term development of the hydroacoustic data processing

Group of Scientific Experts Technical Tests [Dahlman (2020)]

- Group of Scientific Experts (GSE) proposal for experiments including multi-national contribution of seismic sensor data, distributed (national level to provide Level I data) and centralized (data centre to provide Level II data) data processing.
- GSE Technical Tests GSETT-1 to GSETT-3 conducted during the period 1984 to beyond the final test-ban negotiations and the agreement in 1996 on the Comprehensive Nuclear-Test-Ban Treaty (CTBT).
- Features of the GSETT-3 system included:
 - provide rapid acquisition and processing of data from a global network of seismic sensors and process this data at a central facility
 - provide as much automation as possible in the collection, processing, and distribution of data
 - establish a monitoring system architecture flexible enough to allow any technical modifications and improvements that might be needed in the future
- While GSETT-3 was limited to seismic monitoring, its system design would be flexible enough to incorporate the collection, archiving, and distribution of data from non-seismic techniques, such as hydroacoustics, infrasound, and radionuclide.
- United States offered to host a Prototype International Data Center (PIDC) project at the Center for Monitoring Research (CMR) in Arlington, Virginia, USA. This was running the GSETT-3 experiment at the time the Treaty was negotiated, starting in 1995.
- GSETT-3 continued during the initial build-up of the International Monitoring System (IMS) starting in 1997, at the Provisional Technical Secretariat (PTS) of the Prep. Comm. for the Comprehensive Nuclear-Test-Ban Treaty Organization (CTBTO) in Vienna.
- The PIDC project continued at the CMR in Arlington until March 2000.

Early implementation of IDC processing algorithm at CTBTO

- The United States generously donated the software and associated documentation to the PTS.
- The first delivery of the automatic processing algorithm (R1) at CTBT IDC was mainly configured for seismic network processing [Gerstoft (2000)].
- The CTBT IMS hydroacoustic network was routinely monitored during the R1 release and was composed of:
 - Two hydrophones WK30 and WK31 at Wake Island, Pacific Ocean, located around 240 km apart.
 - One T-station VIB at Queens Island, Canada, with one vertical component.
- The CTBT automatic processing algorithm (R1) was still in a development phase and was mainly composed of:
 - Detection and Feature eXtraction (DFX)
 - Station Processing (StaPro)
 - Global Association (GA)
- R1 release was operational 15 May 1998 to 28 May 1999 and a later version was running at PIDC in Arlington, USA
- Release R2 of the automatic processing algorithm was transferred from PIDC in May 1999.
- Lessons carried forward as the IDC moved towards its final goal of building a system capable of fulfilling the relevant Treaty obligations.
- Release 3 more complicated and included more auxiliary stations.

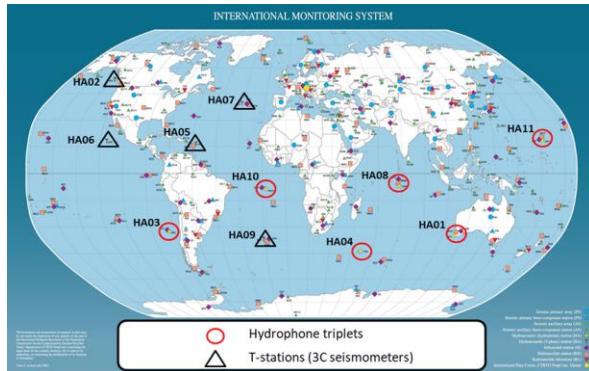
Ad-hoc Expert Group

- Release 3 of the IDC application software was installed, and development and maintenance taken over by IDC.
- Ad-hoc Expert Group on:
 - Evaluation of Hydroacoustic Data Processing at the International Data Centre.
- A total of 3 meetings in 2002 and 2003 at the premises of the CTBTO Preparatory Commission.
- Recommended 6 High Priority Areas
 - Station-specific processing parameters
 - Multichannel processing of triad data
 - Usage of T and H phases in event definition and location
 - Modelling of travel time and transmission loss
 - Characterization of arrival time is critical to location (refinement of PWT)
 - Spectrogram tool for interactive phase identification.

Disclaimer: The views expressed on this presentation are those of the author and do not necessarily reflect the view of the CTBTO



Certification of Hydroacoustic Stations



Treaty Number	Certification	IDC Operation	Station Type
HA01	10-DEC-2001	25-APR-2002	Hydrophone
HA02	20-DEC-2006	29-JAN-2007	T-station
HA03	14-NOV-2003	09-JUL-2003	Hydrophone
HA04	19-JUN-2017	02-OCT-2003	Hydrophone
HA05	30-JAN-2002	06-MAR-2002	T-station
HA06	22-DEC-2005	16-MAR-2006	T-station
HA07	21-NOV-2005	28-JUL-2005	T-station
HA08	18-DEC-2000	18-OCT-2001	Hydrophone
HA09	22-DEC-2004	23-MAR-2005	T-station
HA10	15-DEC-2004	23-MAR-2005	Hydrophone
HA11	08-JUN-2007	17-DEC-2007	Hydrophone

- Hydroacoustic stations deployed during the period 2001-2007
- Gradual increase in number of sensors providing data
- All hydroacoustic stations provided data to the IDC Operation

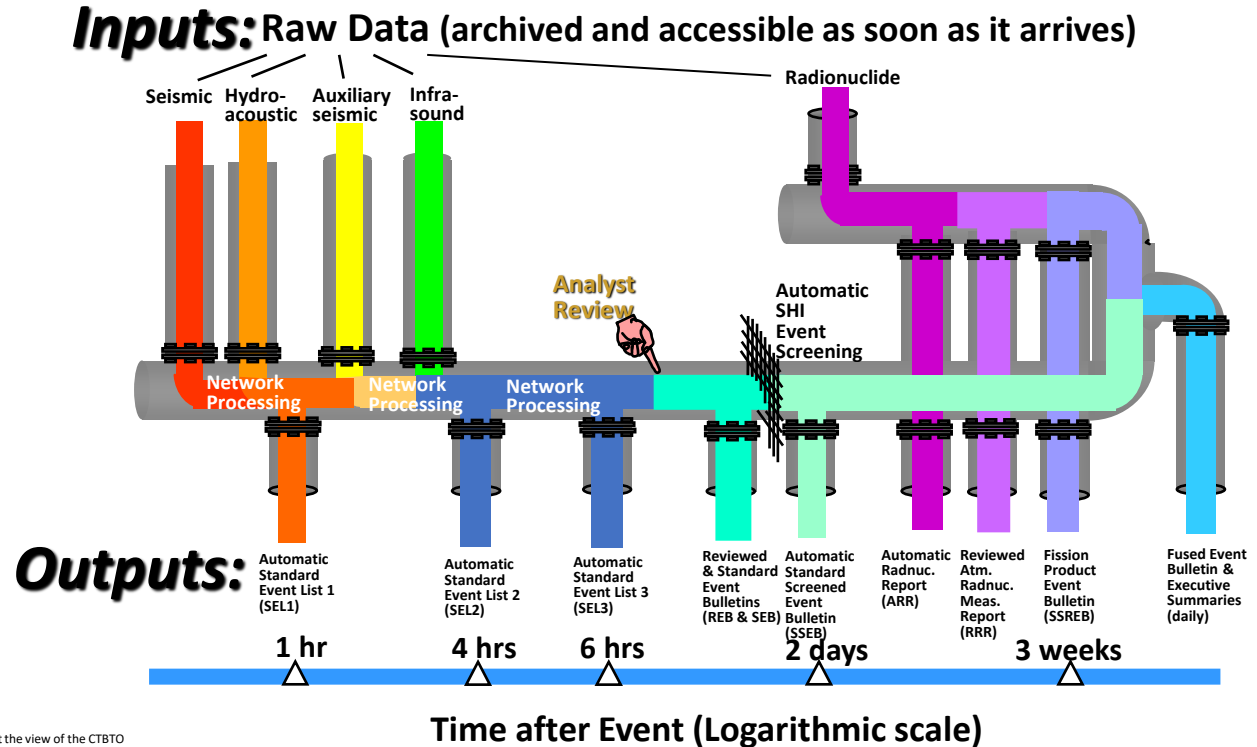
Disclaimer: The views expressed on this presentation are those of the author and do not necessarily reflect the view of the CTBTO

Source for table: [DOTS (2021)]

Schematic of overall flow of IMS data from the three technologies, processing steps, and standard products of the IDC.

Hydroacoustic Processing Algorithms

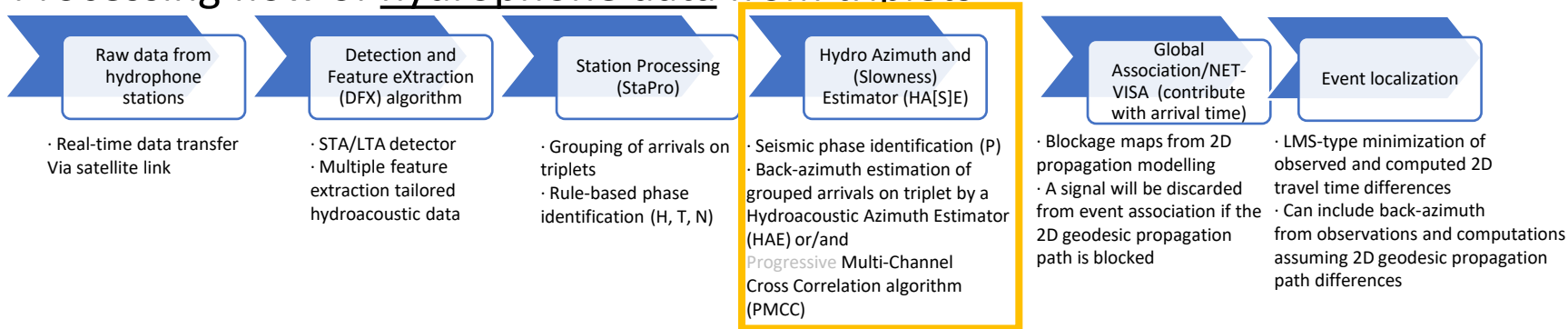
- Detection Feature eXtract (DFX)
- Station Processing (StaPro)
- Hydro Azimuth and (Slowness) Estimator (HAE/HASE)
- Network Processing by Global Association (GA) and NET-VISA
- Interactive review Azimuth and slowness (HART)



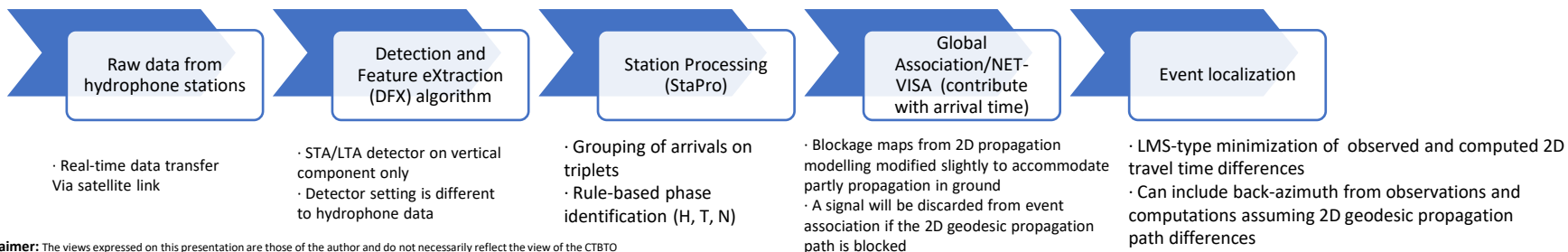
Disclaimer: The views expressed on this presentation are those of the author and do not necessarily reflect the view of the CTBTO

Automatic Processing Software Components

Processing flow of hydrophone data from triplets



Processing flow of seismic data from T-stations



Enhancement of Hydroacoustic Processing [Graeber (2006, 2006a)]

- Computation of Travel Time and Transmission Loss
 - Computations along Nx2D radials from the CTBT IMS hydroacoustic stations.
 - Seasonal varying oceanographic database information.
 - Ocean acoustic propagation model KRAKEN.
- Detection and Feature eXtraction
 - IDC to reverse-engineer *libhydro* to fulfil obligation, porting to other platforms and development of new tools.
 - Calculation of multiple time metrics (arrival, start, termination, peak, probability weighted etc).
 - Cepstral analysis to identify delayed echoes from bubble pulse oscillations from in-ocean explosions.
 - Enlarged frequency processing band to enhance automatic phase identification.

Enhancement of Hydroacoustic Processing [Prior (2008, 2008a, 2011), Tuma (2016), Heaney (2017)]

- **Phase identification**
 - Tuning of rule based phase identification based on extensive data analysis.
 - Fewer wrongly identified H-phases that should have been identified as T-phases.
 - Impact on automatic network processing as H-phases contribute and T-phases do not, i.e., fewer false events based on H-phases.
 - Enhanced rule-set for H-phase identification (number of frequency bands and thinness added to the rules for identifying H-phases) [Prior (2008)].
 - First reported attempt to introduce Neural Net and Support Vector Machines for signal phase identification [Prior (2008a), Tuma (2016)].
 - Identification of signal detections that were blocked by the Global Association algorithm (2-dimensional blockage maps) but were detected because of 3-dimensional propagation effects justified by high-fidelity 3-dimensional modelling of ocean global-scale signal propagation – [Heaney (2017)].

- **Multi-Channel Processing/Azimuth and Slowness Estimation**
 - Refinement of hydrophone locations to eliminate bias in azimuth and apparent wave speed residuals.
 - Introduction of PMCC-like coherent processing of hydrophone triads (HASE) to estimate back azimuth and apparent wave speed for H, T, N and P phases.
 - Introduction of DTK(G)PMCC stand-alone algorithm for signal detection, estimate of back azimuth and slowness for hydrophone triplets.

Enhancement of Hydroacoustic Rule Based phase identification (StaPro)

- Frequency band:
 - LFB: 6-12 Hz
 - HFB: 64-100 Hz
- No. Bands
 - Number of processing bands
- Thinness (dB)
 - $SUM(\text{peak_level} - \text{total_energy}) / \text{No. Bands}$
- Energy Ratio (dB)
 - $\text{total_energy (HFB)} - \text{total_energy (LFB)}$
- Time Spread:
 - $\text{total_spread (LFB)}$
- Crossing Density:
 - $\text{num_cross (LFB)} / \text{Duration(LFB)}$
- Fractional Time:
 - $\text{total_time (LFB)} / \text{Duration(LFB)}$
- Duration:
 - $\text{termination_time(LFB)} - \text{onset_time(LFB)}$

Attribute	H phase (Step 1)	T phase (Step 2)	N phase (Step 3)	N phase (Step 4)	H phase (Step 5)
No. Bands	> 6				H phase if neither T nor N phases
Thinness	> 0				
Energy Ratio		< 5	< 0.1	Missing or	
Time Spread		> 3 s	> 35 s	Missing or	
Crossing Density		> 8 s ⁻¹	> 40 s ⁻¹	Missing or	
Fractional Time			< 0.2	Missing or	
Duration			< 6 s	Missing	

Disclaimer: The views expressed on this presentation are those of the author and do not necessarily reflect the view of the CTBTO

Enhancement of Hydroacoustic Rule based phase identification (HASE/StaPro)

Seismic Phase if:

Energy Ratio in dB

$(LBF - MFB) > 12$

- Low Frequency Band (LBF) centered on 1.5 Hz
- Medium Frequency Band (MBF) centered on 3.5 Hz

Slowness (S)

$S \leq 30$ s/degree (corresponding to apparent velocity of 3.7 km/s)

Hydroacoustic Phase if:

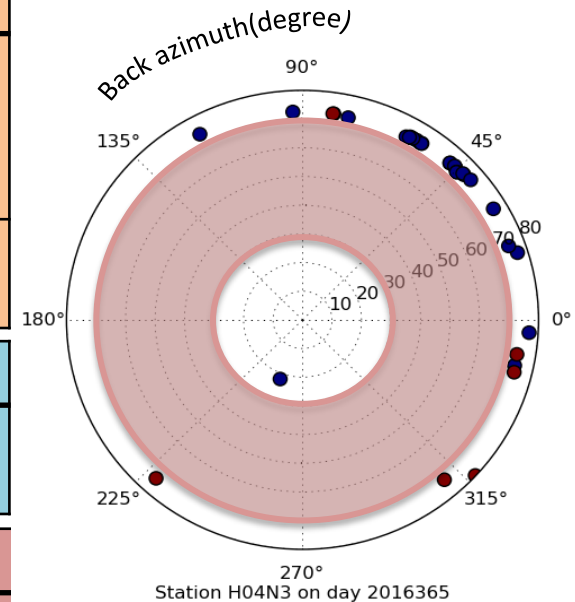
Slowness (S)

$S \geq 70$ s/degree (corresponding to apparent velocity of 1.6 km/s)

Rejected if:

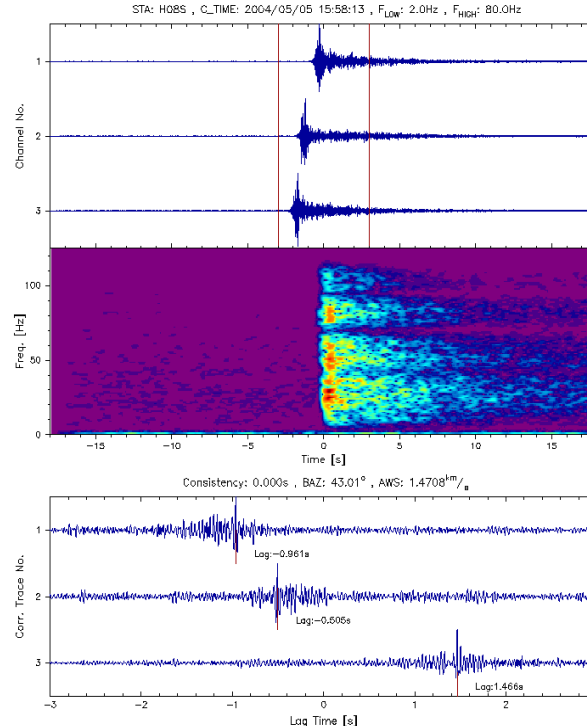
Slowness (S)

$30 \text{ s/degree} < S < 70 \text{ s/degree}$

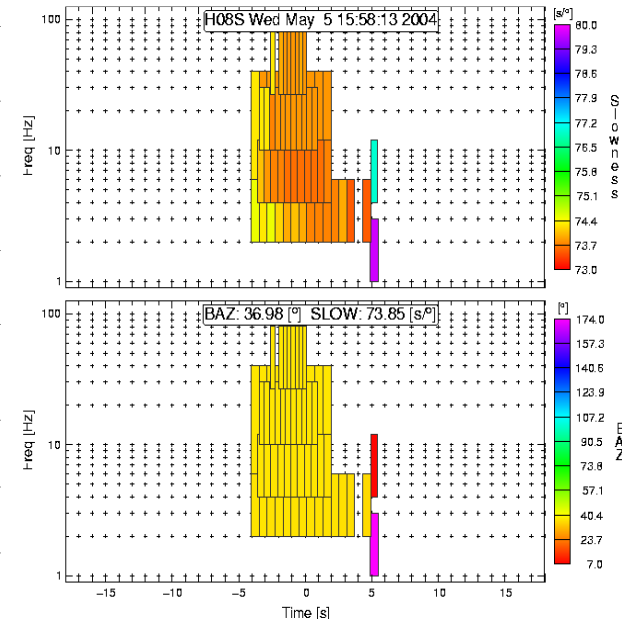


HASE – Hydroacoustic Azimuth and Slowness Estimator [Graeber (2004)]

- Bay of Bengal Event, 05/05/2004.
- Raw time series recorded on three hydrophones at H08S (upper left) and corresponding calibrated spectrogram (middle left).
- Cross-correlation of hydrophone time series (lower left).
- Time-frequency processing of cross-correlation to obtain slowness and back azimuth (upper and lower right respectively).
- Uniform color distribution across time-frequency cells indicate consistent estimate of slowness and back azimuth.



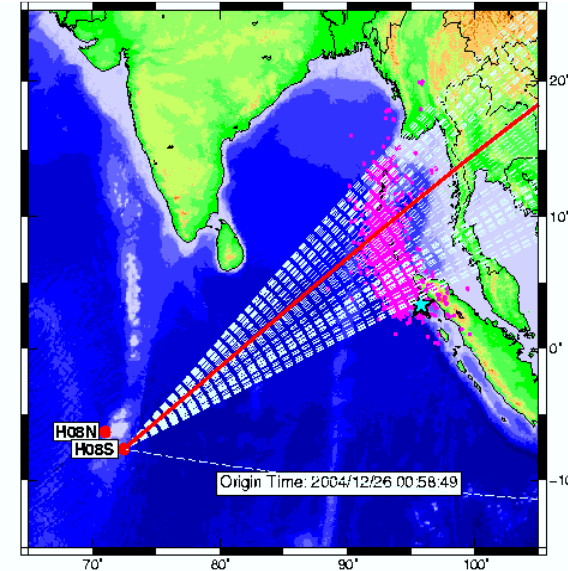
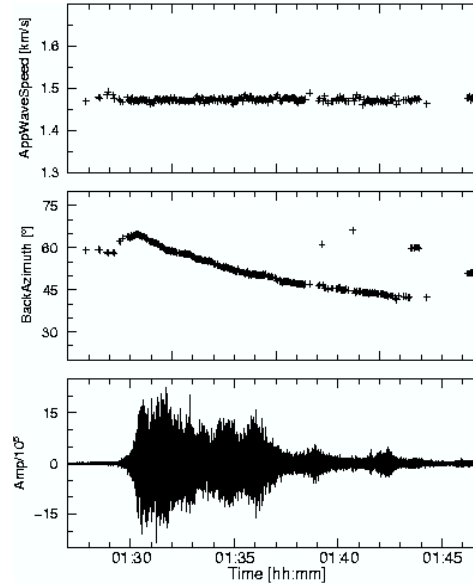
Sliding correlation windows of variable length and use of multiple frequency bands



HASE – Hydroacoustic Azimuth and Slowness Estimator [Graeber (2004)]

T-phases may be of large duration and display large variations in azimuth. In the case, the T-phase from the main shock records rupture propagation along the earthquake fault initially to the South and then mostly to the North.

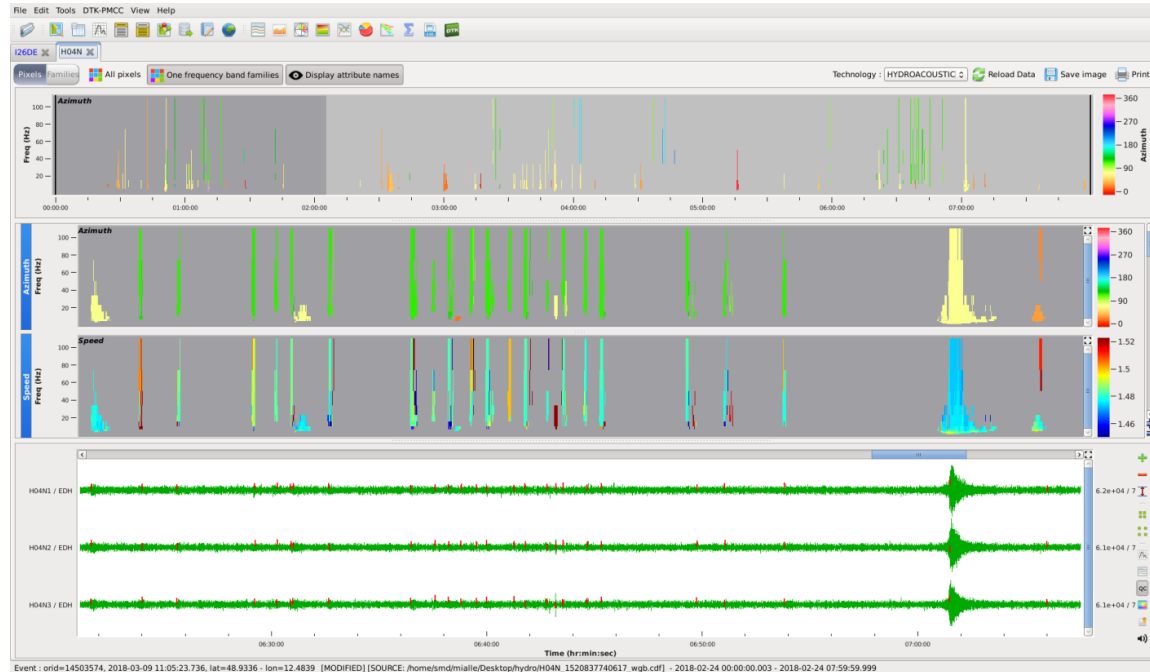
- The Sumatra–Andaman earthquake 26/12/2004 00:58:53 UTC.
- HASE applied to estimate apparent wave speed and back azimuth on H08S time series of duration 20 minutes.
- Time evolution of apparent wave speed (upper left).
- Time evolution of back azimuth (middle left).
- Raw time series (T-phase) recorded on one hydrophone of H08S (lower left).
- Back azimuth interval (white dashed lines), mean back azimuth (red line) and estimated location of ground-to-water wave coupling (magenta dots).



DTK-PMCC – detection and review in IDC LANs with hydroacoustic support in 2018

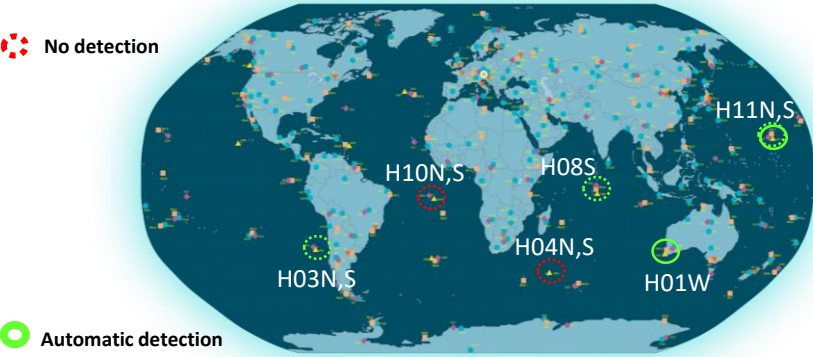
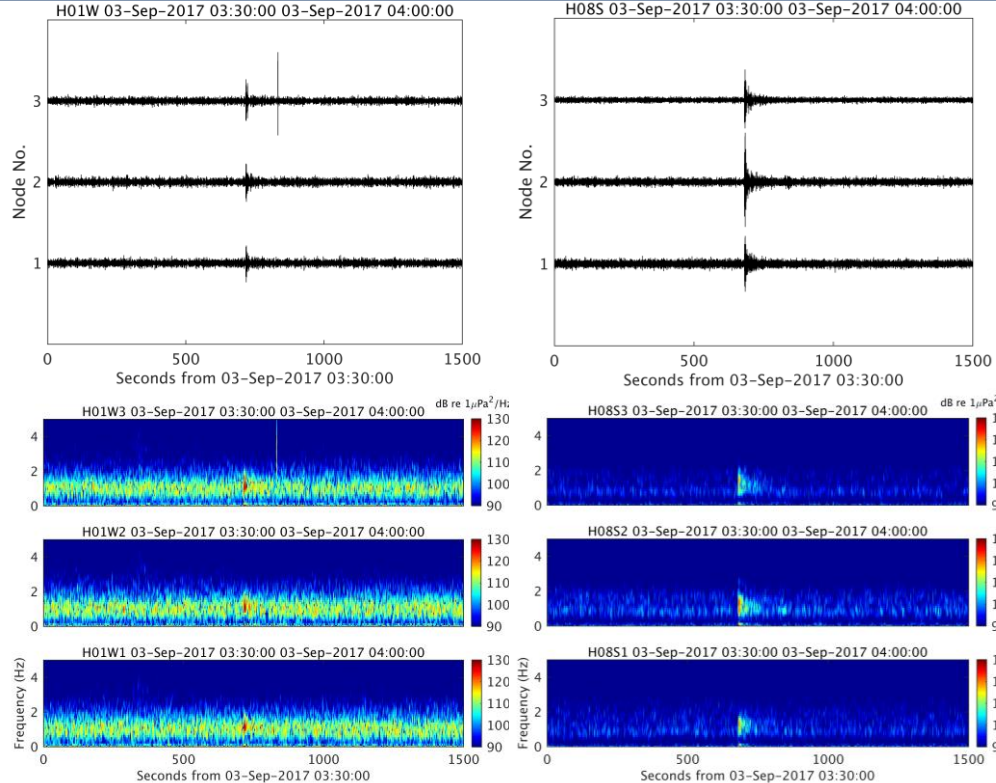
Hydro-acoustic processing (H04N) & automatic detection of technology. Software donated by the French NDC at CEA/DASE

- Station Processing system:
 - Redesigned processing software integrating the Progressive Multi-Channel Correlation method [Cansi (1995, 1997)].
 - Software package allows for 2 modes: stand-alone and integrated in a LAN linked to database.
 - Extended from infrasonic waveform analysis to also include hydroacoustic processing capabilities in 2018.
- DTK-PMCC
 - Detection calculation software from the flow saved on the hard drive. This software contains the core system algorithm.
 - Command line software that can be coupled with interactive interface (DTK-GPMCC) or integrated into an operational pipeline (such as IDC LAN)
- DTK-GPMCC:
 - Software working in interactive or automatic mode, that allows making measurements or visualizing and modifying existing measurements from the raw flow and the automatic detections.
 - DTK-GPMCC is the graphical user interface linked with the DTK-PMCC algorithm. It executes the algorithm, retrieves the results and provides them for further analysis (advanced setting, computation launch, graphical representations, etc...)



Hydroacoustic detection and localization of DPRK6 [Nielsen (2018)]

- Recorded time series at H01W and H08S hydroacoustic station: on 3rd September 2017 (DPRK6).
- Signal received at H01W was detected by the IDC automatic processing system as P-phases while the signal received at H08S was detected manually.
- Calibrated spectrograms of signals received at H01W and H08S hydroacoustic stations on 3rd September 2017.
- Filtering using a 3rd order Butterworth bandpass filter in the band 0.8-4.5 Hz (seismic band).

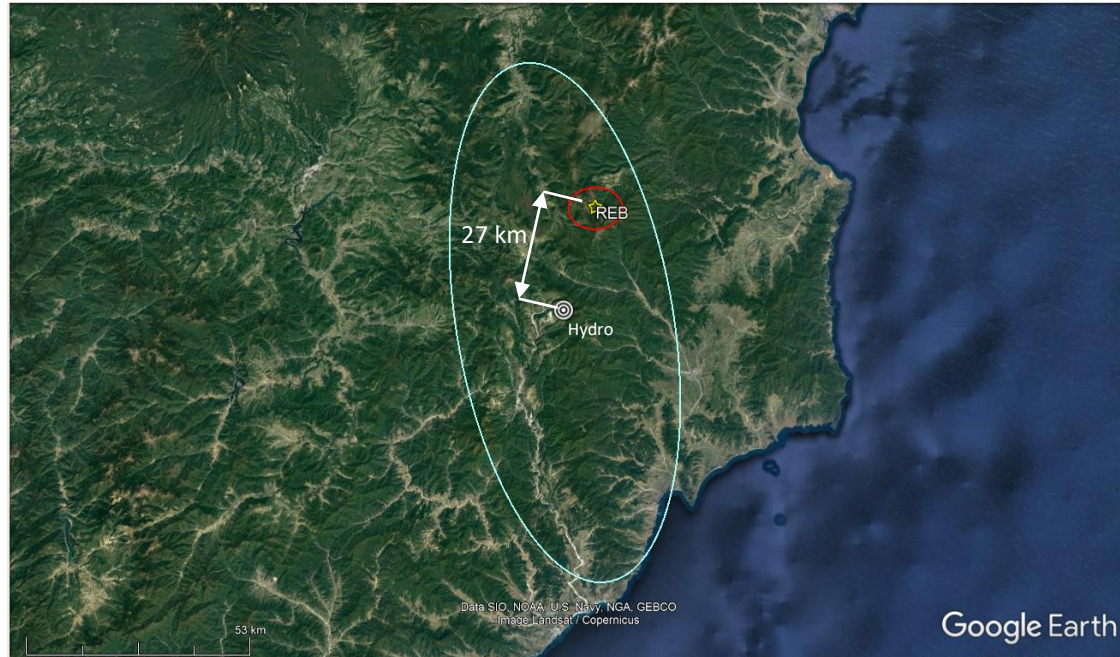


-  No detection
-  Automatic detection
-  Manual detection

Disclaimer: The views expressed on this presentation are those of the author and do not necessarily reflect the view of the CTBTO

Hydroacoustic detection and localization of DPRK6 [Nielsen (2018)]

- Estimate of location and error ellipse using 125 seismic IMS stations (red ellipse) and hydrophone stations only (blue ellipse)
- Difference in event location using 125 seismic IMS stations and hydrophone stations only:
 - Difference: 27 km
- Dimension of location error ellipse using 125 seismic IMS stations:
 - Semi-major error ellipse axis: 6 km
 - Semi-minor error ellipse axis: 5 km
 - Ellipse strike/orientation: 88°
- Dimension of location error ellipse using hydrophone stations only:
 - Semi-major error ellipse axis: 64 km
 - Semi-minor error ellipse axis: 27 km
 - Ellipse strike/orientation: 171 °



Disclaimer: The views expressed on this presentation are those of the author and do not necessarily reflect the view of the CTBTO

Network Processing NET-VISA [Arora (2013)]

- Travel time between any two points on Earth and the attenuation of various frequencies and wave types are not known accurately
- Each detector is subject to local noise that may mask true signals and cause false detections
- Thousands of detections are recorded per day, so the problem of proposing and comparing possible events (subsets of detections) is daunting
- Suggest that an approach based on probabilistic inference and combination of evidence might be effective
- Early tests of global signal associator NET-VISA [Arora (2013)]
- NET-VISA extended to include *hydroacoustic* together with seismic [Arora (2014, 2019), Le Bras (2020)]
- NET-VISA (relies on IDC signal features) and SIG-VISA operating on full waveforms [Moore (2017), Le Bras (2020)]

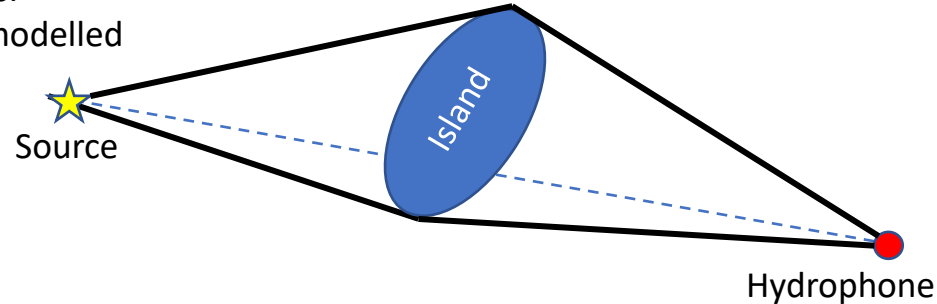
Network Processing. NET- and SIG-VISA [Arora (2013), Moore (2017), Le Bras (2020)]

- Potential use of Machine Learning methods to improve data processing at CTBT IDC
- Outcome of workshop in 2009 was initiation of proof-of-concept of Network Processing:
 - NET-VISA as one-to-one replacement of the Global Association (GA) software using parametric detection data as input
 - SIG-VISA substituting Detection and Feature eXtraction (DFX), Station Processing (StaPro) and GA using raw waveforms as input.
- Both stages of the VISA developments were aimed at a probabilistic framework based on a Bayesian approach instead of the comprehensive exploration of all possible combinations of detections, followed by a heuristic approach to resolve 'conflicts' where a detection is associated to multiple events used in GA.
- Distributions of time, slowness and back azimuth residuals are derived from the large set of reviewed events.
- Expectations:
 - Missed event rate decreases by at least ten percent
 - Better completeness of the events in terms of the number of stations associated to an automatic event
 - Higher productivity of analysts and more in-depth understanding of each event.
- Early tests of global signal associator NET-VISA [Arora (2013)]
- NET-VISA extended to include hydroacoustic together with seismic [Arora (2014, 2019), Le Bras (2020)]

Disclaimer: The views expressed on this presentation are those of the author and do not necessarily reflect the view of the CTBTO

NET-VISA [Arora (2013, 2014, 2019), Le Bras (2019, 2020)]

- NET-VISA hypothetical event location.
- Physics-based, probabilistic model and an inference algorithm.
- Basic components of NET-VISA are a Generative Model (GM) and an Inference Algorithm (IA).
- Addition of hydroacoustic to seismic
 - Prior of hydroacoustic H phase event locations uniformly distributed at a rate of one (1) per hour
 - Prior of remaining IDC derived signal features derived from reviewed by-analysts historical data
 - Generative model (Geometrical spreading and absorption in water)
 - Inference by considering all possible combinations of arrivals that maximizes the likelihood for observed events.
 - Possibility of Out-of-Plane (OOP) diffracted arrival modelled in addition to blockage. Probability of detection decreases exponentially with OOP angle.
- NET-VISA migration to operational network.
- Enhancement of automatic event detection from global network using NET-VISA and improved contribution from the hydroacoustic network.



Interactive review of hydroacoustic data

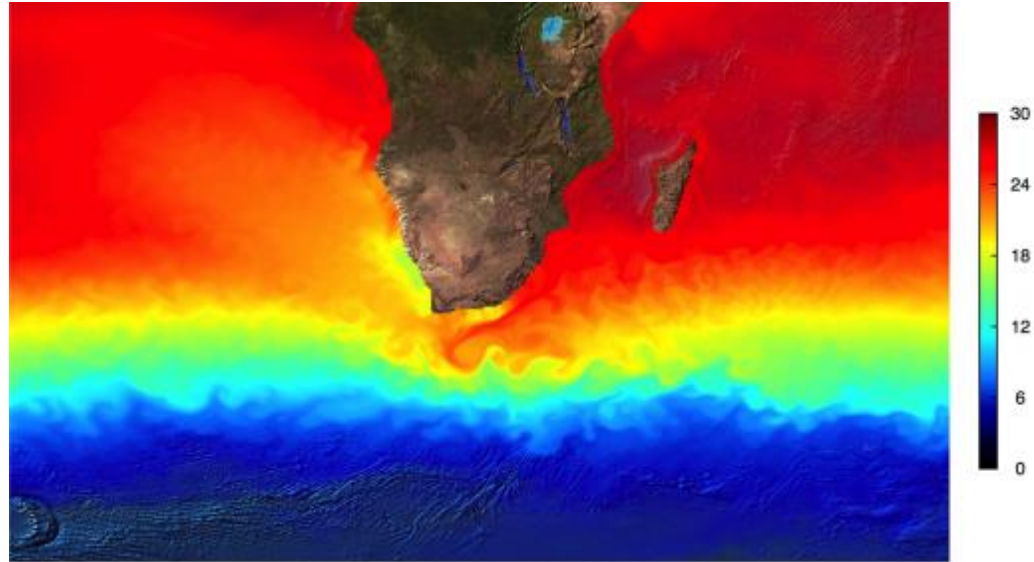
- A large percentage of events in the reviewed event bulletin (REB) contain T phases. The numbers for year 2020 are shown below:

	Total number of events	Events with T phases	Events with H phases
2020	34195	8479 (24.80%)	23 (0.07%)
2019	35285	8392 (23.78%)	13 (0.04%)

- T phases do not contribute to the location of a event but are observed for small events and may lead to the building of mixed seismic-hydroacoustic events in the REB which would be missed by a seismic-only network. They contribute to about a quarter of the REB events.
- Events with H phases are confirmed a few times within a year. H phases contribute to the location of the event. These events are in-water but may also be recorded by on-land seismometers.
- The large REB bulletin accumulated over twenty years provides a high-quality record of seismo-acoustic events which contributes to the advancement of knowledge in this area.
- Another major contribution of the hydroacoustic network is the post-analysis automatic screening step. If an event is shallow and its epicentre in ocean deeper than 500m, it can be safely classified as natural if no H phases that should be observed (i.e. with no blocked path to the station) are observed.

Oceanographic Modelling for Hydroacoustic Processing 2016-2021 [Heaney (2016)]

- Meso-scale (10-100 km spatial scale) oceanographic eddies are known to impact ocean acoustic signal propagation.
- The spatial and temporal behaviour of eddies are predictable by global sophisticated oceanographic models.
- Computational intensive and may require nesting to obtain sufficient resolution.
- Essential input to global-scale 3D acoustic signal propagation models to predict arrivals at IMS hydroacoustic stations.
- The oceanographic models also predict ocean current which may cause cyclic movements of individual hydrophones in the hydroacoustic triplets.
- Knowledge of local ocean current may allow for corrections of temporal dependent location of hydrophones in the IDC processing.

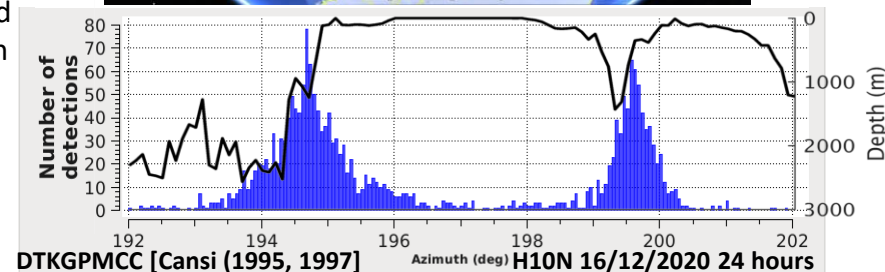
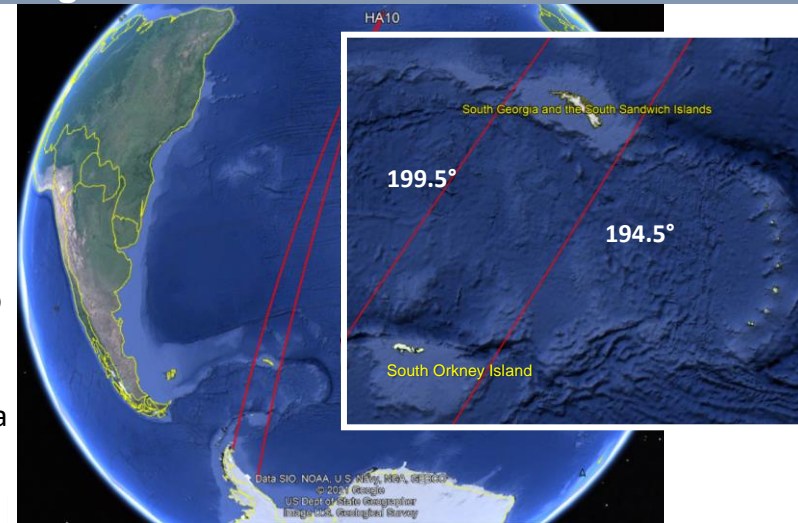


ECCO2 Sea Surface Temperature

Disclaimer: The views expressed on this presentation are those of the author and do not necessarily reflect the view of the CTBTO

Observed 3D diffraction of signals

- Sound in the southern Atlantic ocean generated by earthquakes in the region between South Georgia and South Orkney Island is detected at H10N [Heaney (2017)].
- The underwater acoustic path is close to blocked for azimuths 194.5° between 199.5° by the South Georgia Island and its underwater plateau.
- The arrivals are not identified as T-phases propagating in the ground and coupled into the ocean North of South Georgia as the travel times correspond to signals travelling at the ocean sound speed.
- Relative narrow trench-like underwater acoustic paths at azimuths 194.5° and 199.5° (red lines in upper panels) where sound can escape around South Georgia Island.
- A typical number of detections at H10N for 24 hours of acquisition is shown in the lower panel with a distribution centred around azimuths of 194.5° and 199.5° . Minimum water depth along 500-km radials centred around South Georgia Island is shown as the black line.
- The detection of signals originating from behind and blocked by South Georgia Island can be explained by 3D diffraction of the signals around South Georgia Island.

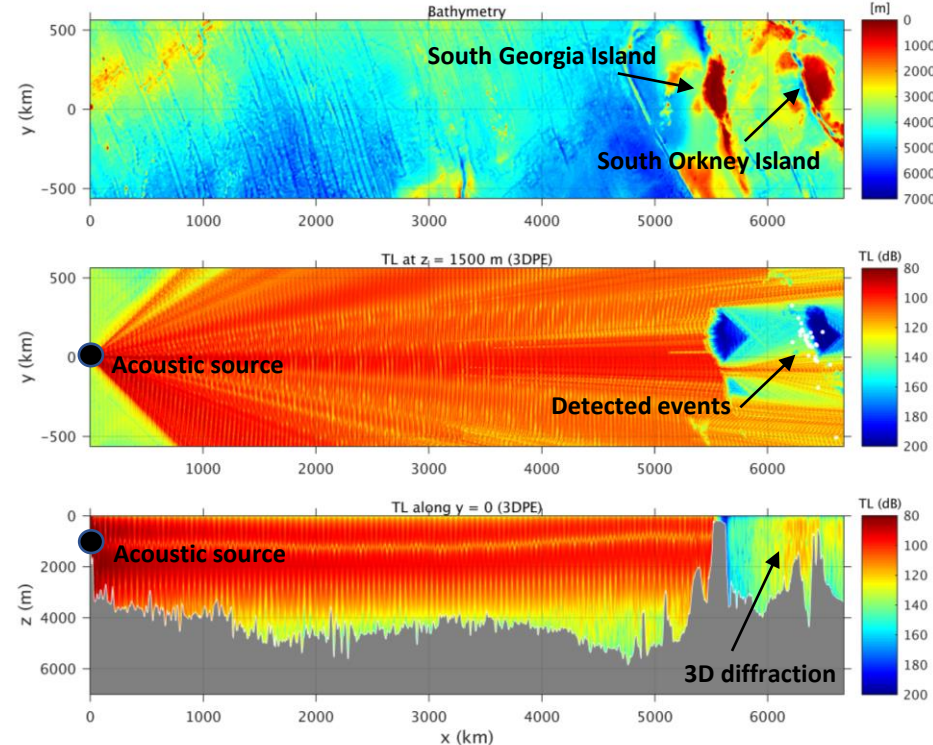


Modelling of 3D diffraction of signals

3D Parabolic Equation model SSF PE [Lin (2013), Kushida (2020)]

The authors are gratefully acknowledged making the 3D SSF PE available

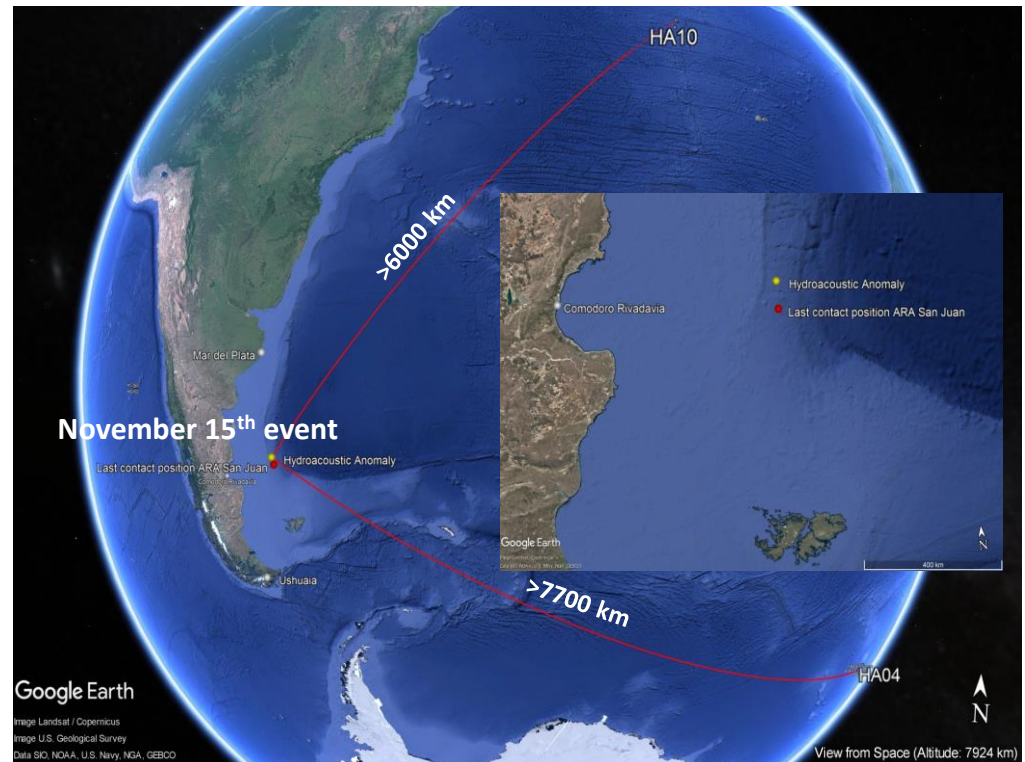
- GEBCO bathymetry swath along a geodesic path from triplet H10N at (0,0) to a location close to South Orkney Island (6850,0) passing through South Georgia Island (upper panel).
- Computation of 3D underwater signal propagation presented as TL at 5 Hz using the SSF PE [Lin (2013), Kushida (2020)] from H10N towards South Orkney Island at a depth of 1500 m (middle panel).
- At least 32 events in the period 2006-2014 detected and stored in the Standard Event Level 3 from the automatic processing although line-of-sight blockage by South Georgia Island (white dots beyond 6000 km).
- Diffraction of sound around South Georgia can make T-phase arrivals visible at H10N when blockage based on 2D computations predict they would not be seen (middle panel) [Heaney (2017)].
- Diffraction fills the entire water column behind South Georgia making it possible to detect the sound source at any receiver depth.
- [GEBCO Digital Atlas, Copernicus Marine Service Information]



Modelling of 3D effects of signals

Refraction and diffraction from seamounts, Islands and continents

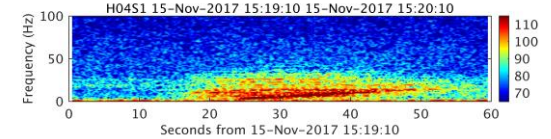
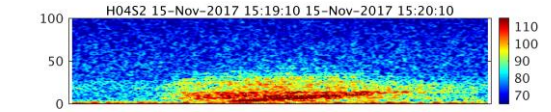
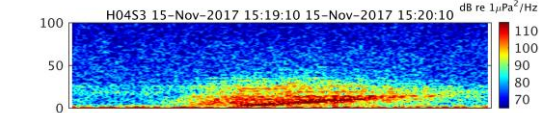
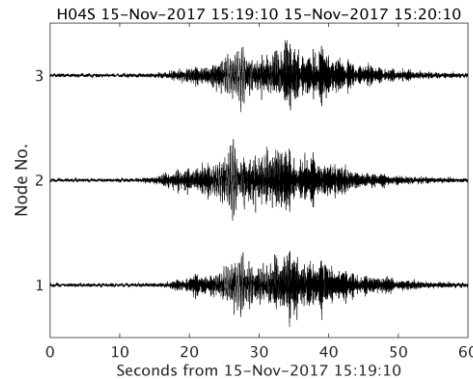
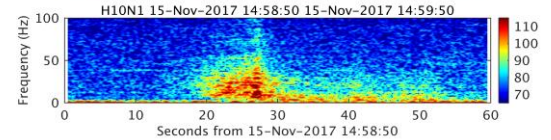
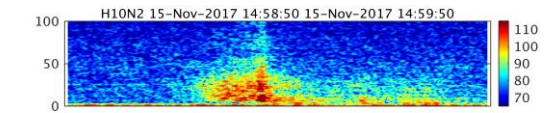
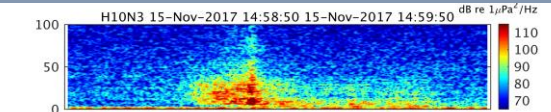
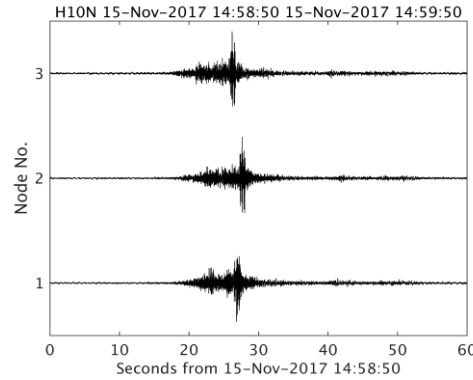
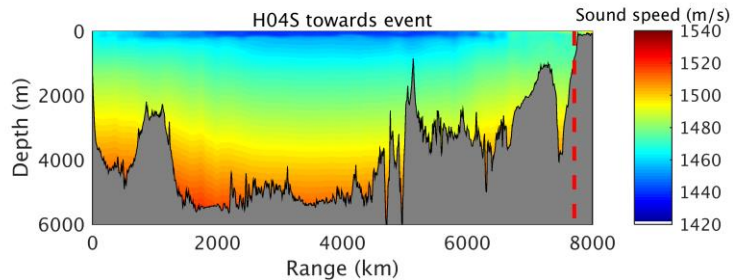
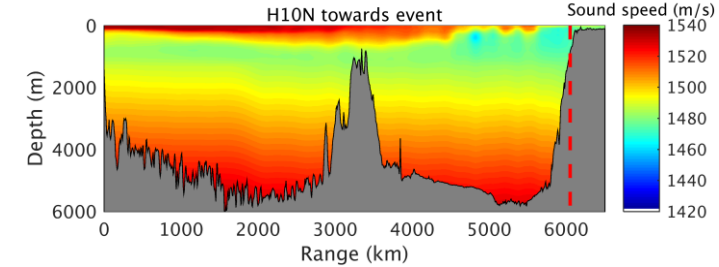
- Signal of unknown origin detected on November 15th 2017 in the vicinity of the last known position of the lost Argentine submarine ARA San Juan.
- Controlled explosion test conducted by Argentine Navy on December 1st 2017, with source position and time information.
- The November 15th signal and the December 1st test source were both detected on CTBT IMS hydrophone stations HA10 and HA04.



Disclaimer: The views expressed on this presentation are those of the author and do not necessarily reflect the view of the CTBTO

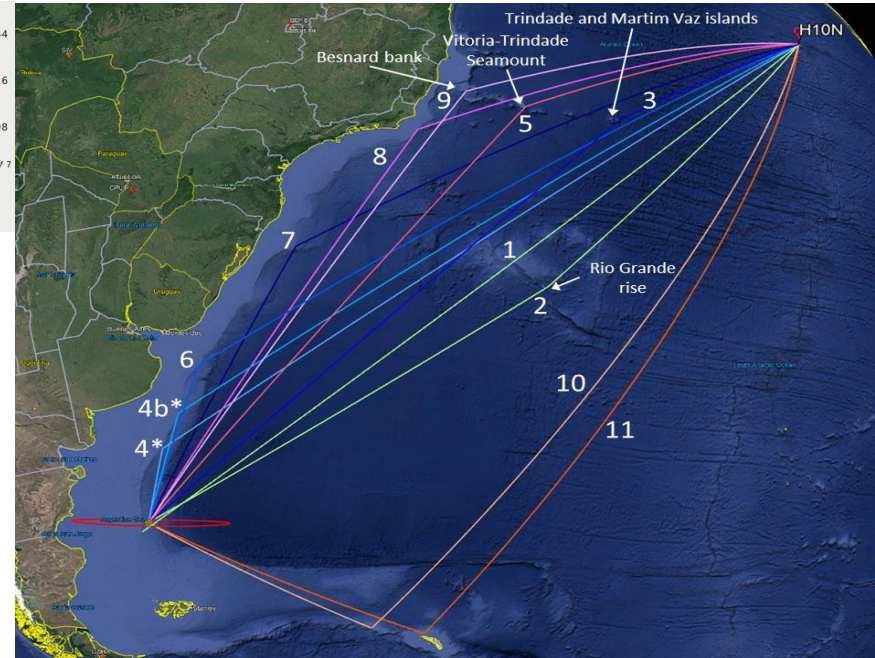
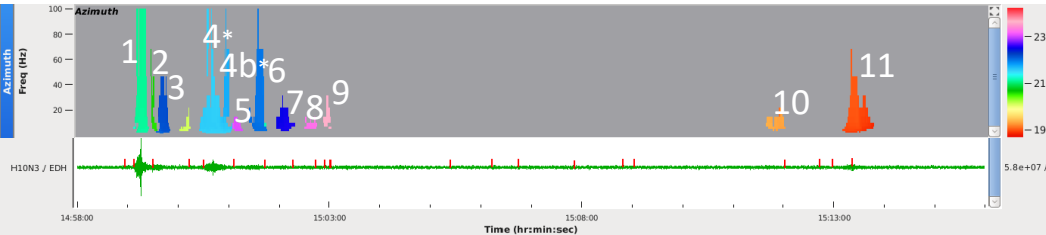
Observation of signal variability recorded at two hydrophone stations from the same event

Refraction and diffraction from seamounts, Islands and continents



Disclaimer: The views expressed on this presentation are those of the author and do not necessarily reflect the view of the CTBTO

Multiple arrivals at H10N



- November 15th signal received on H10N and analyzed using a Progressive Multi Channel Cross-correlation (PMCC) processing algorithm [Cansi (1995, 1997)].
- A sequence of 10 late arrivals following the direct main arrival (path number 1) is identified by analyzing a 15 min time window after the main arrival.
- Late arrivals are attributed to reflections off underwater bathymetric features [Vergoz (2021), Dall'Osto (2019, 2019a)].

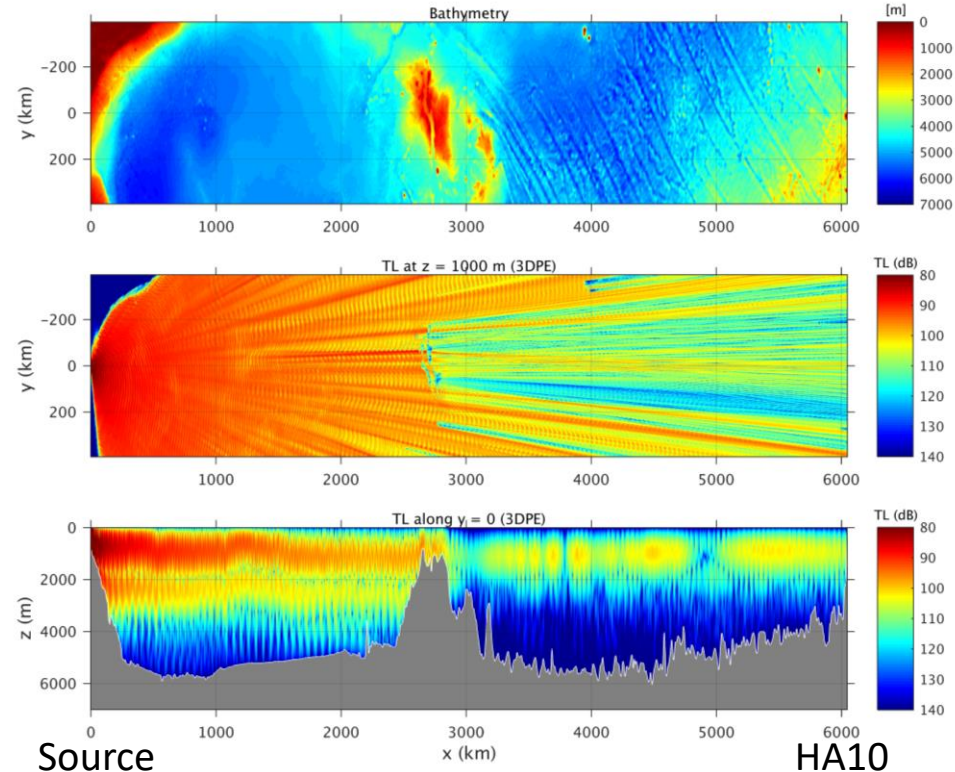
Disclaimer: The views expressed on this presentation are those of the author and do not necessarily reflect the view of the CTBTO

Modelling of 3D refraction and diffraction of signals

Refraction and diffraction from seamounts, Islands and continents

3D Parabolic Equation model SSF PE [Lin (2013), Kushida (2020)]
The authors are gratefully acknowledged making the 3D SSF PE available

- The in-water acoustic anomaly associated with the loss of ARA San Juan was detected at the hydrophone station HA10.
- Horizontally refracted arrivals from the same event were detected up to 15 minutes after the primary arrival following the geodesic propagation path.
- Refraction and diffraction can be observed from the top of Rio Grande Rise (middle panel).
- The acoustic signal propagates in the SOFAR channel, interacts with the Rio Grande Rise and reflected off the ocean bottom to pass the Rise. The signal is again trapped in the SOFAR after the Rise (lower panel).
- The acoustic signal propagating in the ocean after the Rio Grande Rise is a combination of 3D refracted and diffracted propagation paths.

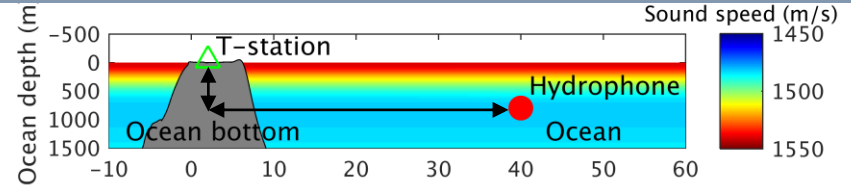


Disclaimer: The views expressed on this presentation are those of the author and do not necessarily reflect the view of the CTBTO

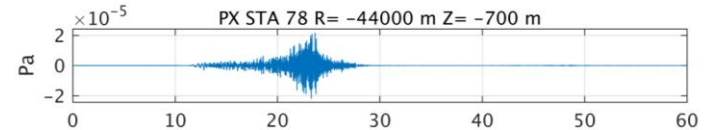
Concept of estimating transfer function from in-ocean to in-ground event

Detection of in-ocean events at on-land seismometers (modelling) [Tromp (2008), Stevens (2020)].

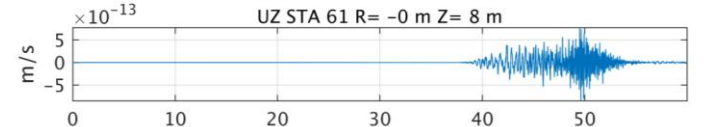
- Difficult to associate in-ocean events to signals recorded at the CTBT IMS on-land T-stations because of high ambient noise levels.
- In-ocean events are observed in recordings from on-land seismometers at different locations than CTBT IMS T-stations.
- Conversion from in-water pressure to in-ground seismic signals at T-stations may reduce or eliminate evidence of an in-ocean event.
- Accurate computation of the transfer function (Greens function) from in-water to in-ground signals may preserve these evidences.
- Convolution of a seismic signal recorded at a T-station with this transfer function may recover features of an in-ocean event at a virtual hydrophone closely located.



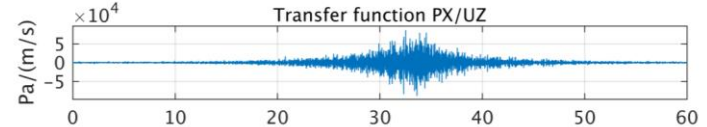
Modelled Pressure



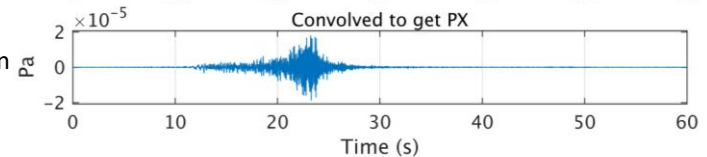
Vertical velocity modelled directly



Modelled Transfer function

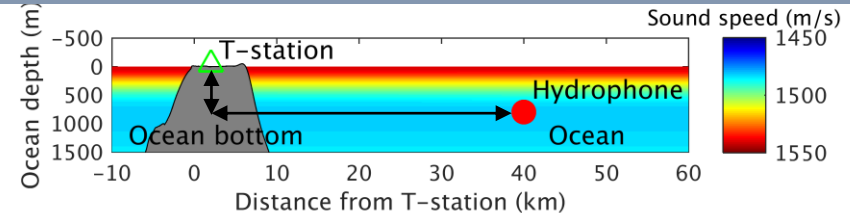


Pressure estimated from transfer function and model vertical velocity

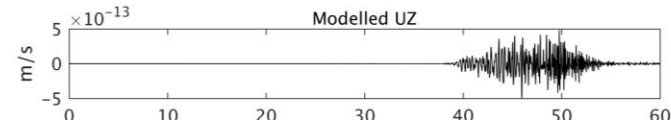


Estimate signal at virtual seismometer based on modelled transfer function

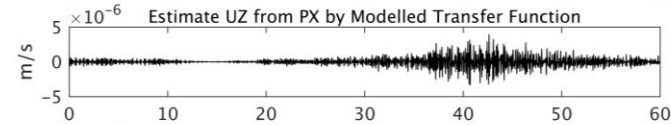
- Event recorded at the CTBT IMS hydrophone station H11N close to Wake Island and the close-to-located WAKE seismometer.
- The transfer function of an in-water pressure signal converted to an in-ground seismic signal is computed by the SPECFEM2D [Tromp (2008), Stevens (2020)].
- Model-based estimate of a virtual hydrophone signal by convolution of the modelled transfer function with the recorded vertical component of the seismometer data.
- Experience reveals that it is more demanding to estimate the signal at a virtual hydrophone than a virtual seismometer.
- Improved similarity between estimates and observations of the virtual signals are sought by an inversion for optimum underwater environmental parameters.
- This is a new project and is still in progress.



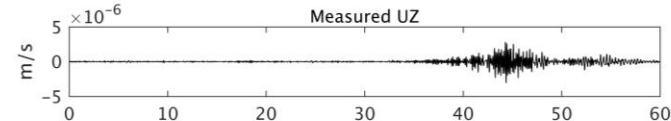
Vertical velocity modelled directly



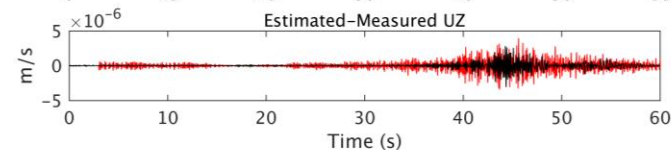
Measured pressure convolved with modelled transfer function to estimated velocity



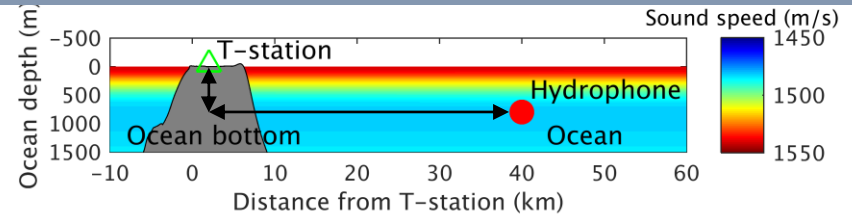
Measured vertical velocity on seismometer



Estimated (red) and measured (black) vertical velocity



Estimate signal at virtual hydrophone based on modelled transfer function



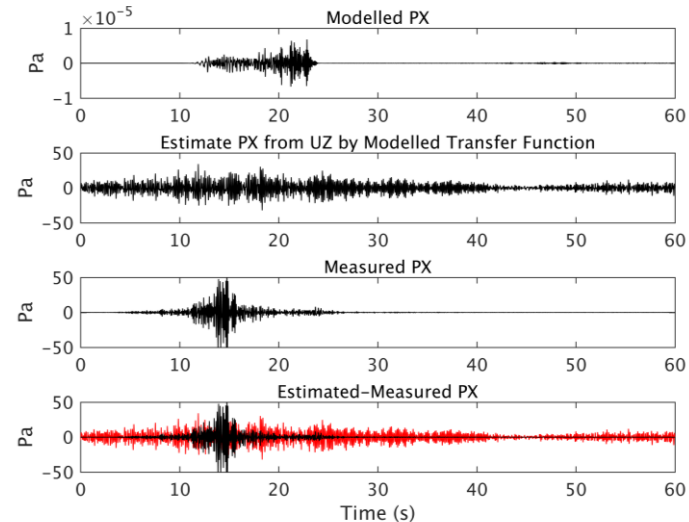
- Event recorded at the CTBT IMS hydrophone station H11N close to Wake Island and the close-to-located WAKE seismometer.
- The transfer function of an in-water pressure signal converted to an in-ground seismic signal is computed by the SPECFEM2D [Tromp (2008), Stevens (2020)].
- Model-based estimate of a virtual hydrophone signal by convolution of the modelled transfer function with the recorded vertical component of the seismometer data.
- Experience reveals that it is more demanding to estimate the signal at a virtual hydrophone than a virtual seismometer.
- Improved similarity between estimates and observations of the virtual signals are sought by an inversion for optimum underwater environmental parameters.
- This is a new project and is still in progress.

Pressure modelled directly

Measured velocity convolved with modelled transfer function to estimated pressure

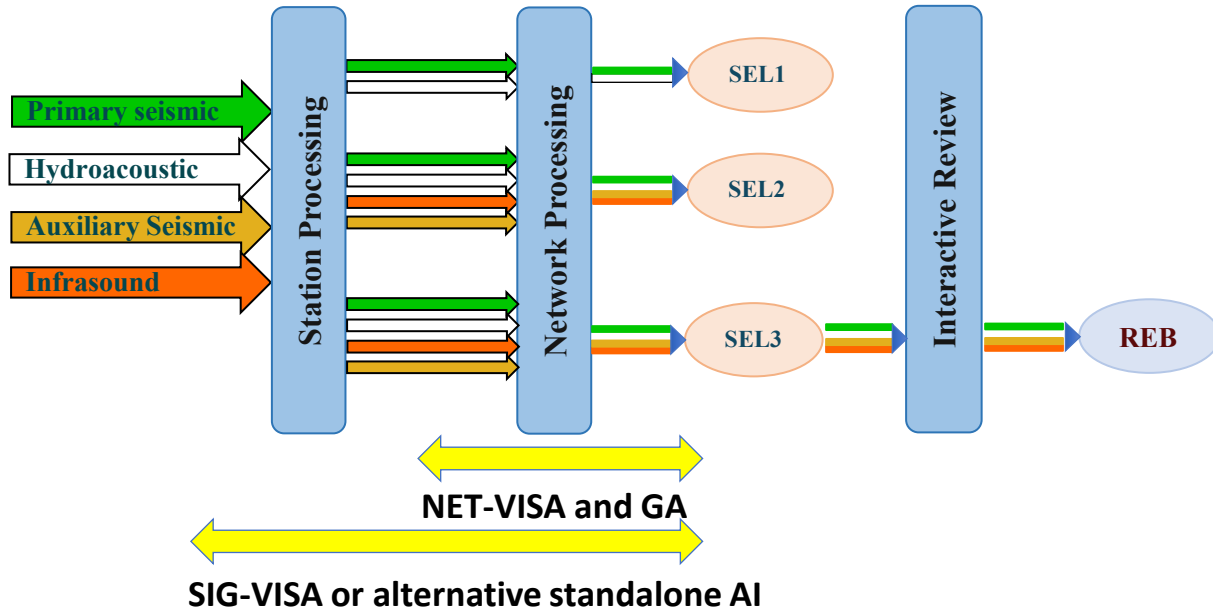
Measured pressure on hydrophone

Estimated (red) and measured (black) pressure



Enhancement of Hydroacoustic Processing

- Initiate exploitation of oceanographic, seismo-acoustic and 3-dimensional ocean signal propagation modelling results (phase conversion, enhancement of blockage maps, travel time tables, probability of detection and estimates of back azimuth).
- Provide rigorous physical basis for predicting and interpreting hydroacoustic signals to train and assist in evaluating observations.
- DTK(G)PMCC migration to operational network – quick long-term station performance assessment, evaluate if events are pertinent to CTBTO (trace back repetitive events as an example)



Near Future

- Implementation of 3-dimensional ocean signal propagation modelling results as part of the automatic signal processing of hydroacoustic data and to assist analysts in interpreting recorded signals on the CTBT IMS hydroacoustic network
- Assess the possibility of using high-fidelity seismo-acoustic models to predict the conversion of in-ocean propagating pressure waves to in-ground propagating seismic waves to enhance performance and utilization of the CTBT IMS hydroacoustic T-stations
- Finale report, PAGEOPH paper by Leidos.
- Introduction of Machine Learning as part of the automatic processing algorithm to identify and characterize recorded in-water pressure waves at hydrophone stations and in-ground seismic waves at T-stations
- Evaluate necessary size of training of state-of-art Machine Learning algorithms to become part of the automatic processing algorithm and eventually supplement with high-fidelity seismo-acoustic propagation modelling.
- Introduce seismo-acoustic wave propagation physics in Machine Learning algorithms
- Apply Machine Learning algorithms for noise reduction at T-stations

Long-term vision

- Substitute part of or entire automatic processing chain of hydroacoustic data all the way from detection to event screening with feedback between station processing and network processing.

- [1] O. Dahlman, F. Ringdal, J. Mackby and S. Mykkeltveit (2020): The inside story of the Group of Scientific Experts and its key role in developing the CTBT verification regime, The Non-proliferation Review, DOI: 10.1080/10736700.2020.1764717
- [2] P. Gerstoft (2000): Assessment of Release 1 Automatic Processing of Hydroacoustic Data, PTS/IDC – 1999/10, Technical Report
- [3] Database of the Technical Secretariat (DOTS) version 4, CTBTO (2021)
- [4] Ad-hoc Expert Group (2003): Evaluation of Hydroacoustic Data Processing at the International Data Centre, Published by the Provisional Technical Secretariat of the Preparatory Commission for the Comprehensive Nuclear-Test-Ban Treaty Organization, CTBT/EVA/EG-2/1
- [5] F. M. Graeber, J. Coyne, and E. Tomuta (2006a): The Current Status of Hydroacoustic Data Processing at the International Data Centre. 28th Seismic Research Review: Ground-Based Nuclear Explosion Monitoring Technologies, pp. 717-724
- [6] M. K. Prior, O. Meless, P. Bittner, H. Sugioka (2011): Long-Range Detection and Location of Shallow Underwater Explosions Using Deep-Sound-Channel Hydrophones, *IEEE J. Ocean. Eng.* 36, pp.703-715
- [7] F. M. Graeber (2006): A new version of DFX-libhydro for IDC operations, IDC/WI/WD
- [8] F. M. Graeber (2007): A new version of the Hydroacoustic Azimuth and Slowness Estimator (HASE 2.0) featuring automatic identification of seismoacoustic arrivals, IDC/WI/WD
- [9] K.D. Heaney and R.L. Campbell (2016): Three-dimensional parabolic equation modeling of mesoscale eddy deflection, *J. Acoust. Soc. Am.* 139, pp. 918-926.
- [10] P. L. Nielsen, R. Le Bras, M. Zampolli, P. Bittner and G. Haralabus (2018): Localization using P-phases recorded on the CTBT IMS hydroacoustic stations. EGU2018-11836, https://presentations.copernicus.org/EGU2018/EGU2018-11836_presentation.pdf
- [11] R. Le Bras, N. Arora, N. Kushida, P. Mialle, I. Bondar, E. Tomuta, F.K. Alamneh, P. Feitio, M. Villarroel, B. Vera, A. Sudakov, S. Laban, S. Nippres, D. Bowers, S. Russell and T. Taylor (2020): NET-VISA from Cradle to Adulthood. A Machine-Learning Tool for Seismo-Acoustic Automatic Association, *Pure Appl. Geophys.* 2020 <https://doi.org/10.1007/s00024-020-02508-x>
- [12] N. S. Arora, S. Russell, and E. Sudderth (2013): NET-VISA: Network Processing Vertically Integrated Seismic Analysis, *Bull. Seismol. Soc. Am.* 103, pp. 709–729, doi: 10.1785/0120120107
- [13] N. S. Arora, S. Russell, H. A. Kuzma (2019), NET-VISA Software Description Document, Preparatory Commission for the Comprehensive Nuclear Test-Ban Treaty Organization (CTBTO) under Contract No. 2012-2107 and Contract No. 2016-2048

- [14] F.M. Graeber and P.-F. Piserchia (2004): Zones of T-wave excitation in the NE Indian ocean mapped using variations in backazimuth over time obtained from multi-channel correlation of IMS hydrophone triplet data, *Geophys. J. Int.* 158, pp. 239–256
- [15] M. Prior (2008) <http://wiki.idc.ctbto.org/pmwiki/pmwiki.php?n=Hydro.STAPROHonH>
- [16] M. Prior (2008a) <http://wiki.idc.ctbto.org/pmwiki/pmwiki.php?n=Hydro.NeuralPhaseID>
- [17] M. Tuma, V. Rørbech, M. Prior, and C. Igel (2016): Integrated optimization of long-range underwater signal detection, feature extraction, and classification for nuclear treaty monitoring, *IEEE Trans. Geosci. Remote Sens.*, vol. 54, no. 6, pp. 3649-3659, doi: 10.1109/TGRS.2016.2522972
- [18] N. S. Arora and M. Prior (2014): Testing and Enhancing the NET-VISA Software of the Commission Fusion of Seismic and Hydro-Acoustic Propagation, BayesianLogic Publication, https://bayesianlogic.com/publications/2014/05/01/Arora_RMR_14.pdf
- [19] R. Le Bras, N. Arora, N. Kushida, P. Mialle, I. Bondar, E. Tomuta, M. Villarroel, B. Vera, A. Sudakov, S. Laban, S. Nippres, D. Bowers, S. Russell and T. Taylor (2019): The machine-learning tool NET-VISA from cradle to adulthood The next generation system of the IDC and the SnT process. SnT T3.5-14, SnT 2019
- [20] K. Heaney, M. Prior and R.L. Campbell (2017): Bathymetric diffraction of basin-scale hydroacoustic signals, *J. Acoust. Soc. Am.* 141, pp. 878-885
- [21] YT. Lin, T.F. Duda and A.E. Newhall (2013): Three-dimensional sound propagation models using the parabolic equation approximation and the split-step Fourier method, *J. Comput. Acoust.*, 21, DOI: 10.1142/S0218396X1250018X
- [22] N. Kushida, YT Lin, P. Nielsen and R. Le Bras (2020): Acceleration in Acoustic Wave Propagation Modelling using OpenACC/OpenMP and its hybrid for the Global Monitoring System, In: Wienke S., Bhalachandra S. (eds) Accelerator Programming Using Directives. WACCPD 2019. Lecture Notes in Computer Science, vol 12017. Springer, Cham. https://doi.org/10.1007/978-3-030-49943-3_2
- [23] D.A. Moore and S.J. Russell (2017): Signal-based Bayesian Seismic Monitoring, Proceedings of the 20th International Conference on Artificial Intelligence and Statistics (AISTATS) 2017, Fort Lauderdale, Florida, USA. JMLR: W&CP volume 54
- [24] The GEBCO Digital Atlas published by the British Oceanographic Data Centre on behalf of IOC and IHO, https://www.gebco.net/data_and_products/gridded_bathymetry_data/
- [25] E.U. Copernicus Marine Service Information. <http://marine.copernicus.eu/services-portfolio/access-to-products/>

- [26] P. L. Nielsen, M. Zampolli · R. Le Bras, P. Mialle, P. Bittner, A. Poplavskiy, M. Rozhkov, G. Haralabus, E. Tomuta, R. Bell, P. Grenard, T. Taylor and N. Meral Özel (2020): CTBTO's data and analysis pertaining to the search for the missing Argentine submarine ARA San Juan, *Pure Appl. Geophys.* <https://doi.org/10.1007/s00024-020-02445-9>
- [27] Y. Lin, T. Oliveira, P. Nielsen (2019): Three-Dimensional Global Scale Underwater Sound Propagation Modeling, International Hydroacoustics Workshop 2019 (IHW2019), 08 - 11 July, Vienna, VIC
- [28] J. Tromp, D. Komatitsch and Q. Liu (2008): Spectral-Element and Adjoint Methods in Seismology,, *Commun. Comput. Phys.* 3, pp. 1-32. ISSN 1815-2406. Available from <https://geodynamics.org/cig/software/specfem2d>
- [29] J.L. Stevens, J. Hanson, P. Nielsen, M. Zampolli, R. Le Bras, G. Haralabus and S.M. Day (2020): Calculation of Hydroacoustic Propagation and Conversion to Seismic Phases at T-Stations, *Pure Appl. Geophys.* <https://doi.org/10.1007/s00024-020-02556-3>
- [30] R. Heyburn, S. E. J. Nippess and D. Bowers (2016): Seismic and Hydroacoustic Observations from Underwater Explosions off the East Coast of Florida, *Bull. Seism. Soc. Am.*, 108, pp. 3612-3624; doi: 10.1785/0120180105
- [31] Y. Cansi (1995): An automatic seismic event processing for detection and location: the PMCC method, *Geophys. Res. Lett.* 22, pp. 1021-1024
- [32] Y. Cansi and Y. Klinger (1997): An automated data processing method for mini-arrays, *CSEM/EMSC European-Mediterranean Seismological Centre*, NewsLetter 11, pp. 1021-1024
- [33] J. Vergoz, Y. Cansi, Y. Cano and P. Gaillard (2021): Analysis of Hydroacoustic Signals Associated to the Loss of the Argentinian ARA San Juan Submarine, *Pure Appl. Geophys.* <https://doi.org/10.1007/s00024-020-02625-7>
- [34] D. Dall'Osto (2019): How consideration of Horizontal Refraction from the Continental Shelf Break improves Source Triangulation: Application to the Search for the ARA San Juan, *J. Acoust. Soc. Am.* 146, pp. 2104-2112
- [35] D. Dall'Osto (2019a): Reducing Ambiguity in Hydroacoustic Triangulation Through Consideration of Three-Dimensional Propagation Features, presentation T1.3 O9, CTBT: Science and Technology conference https://events.ctbto.org/sites/default/files/2019-06/SnT2019_Book_Of_Abstracts_Web_Version_with_front_cover.pdf
- [36] J. Hanson, R. Le Bras, P. Dysart, D. Brumbaugh, A. Gault, & J. Guern (2001): Operational processing of hydroacoustics at the prototype international data center. *Pure Appl. Geophys.* 158, pp. 425-456, <https://doi.org/10.1007/PL00001190>
- [37] H. Laney, P. Dysart, and H. Freese, D. Brumbaugh, R. Le Bras, and J. Hanson (1999): Automated detection of underwater explosions by the IMS hydroacoustic network, *J. Acoust. Soc. Am.* 105 DOI: 10.1121/1.424952